Evaluation of Marrow Perfusion in the Femoral Head by Dynamic Magnetic Resonance Imaging:

Effect of Venous Occlusion in a Dog Model

Hiroshi Tsukamoto, MD[*,†], **Young S. Kang, MD, PhD**[*,‡], **Lynne C. Jones, MS**[§], **Maria Cova, MD**[*,¶], **Christian J. Herold, MD**[‖], **Elliot McVeigh, PhD**[*], **David S. Hungerford, MD**[§], and **Elias A. Zerhouni, MD**[*]

[*]*Department of Radiology, The Johns Hopkins University School of Medicine, Baltimore, Maryland*
[§]*Department of Orthopedic Surgery, The Johns Hopkins University School of Medicine, Baltimore, Maryland*

Abstract

Rationale and Objectives—There is a continuing need for a greater sensitivity of magnetic resonance imaging (MRI) in the diagnosis of avascular necrosis (AVN). Previously, it was demonstrated that a dynamic MRI method, with gadolinium-DTPA (Gd-DTPA) enhancement, can detect acute changes not seen on spin-echo images after arterial occlusion in a dog model. Because venous congestion appears to be a more directly relevant hemodynamic abnormality in a majority of clinical AVN cases, the authors extended the dynamic MRI technique to study changes in venous occlusion.

Methods—Dynamic MRI of the proximal femur was performed in five adult dogs before and after unilateral ligation of common iliac and lateral circumflex veins. Sixteen sequential gradient-recalled pulse sequence (GRASS) images (time resolution = 45 mseconds, echo time = 9 mseconds, flip angle = 65°) were obtained immediately after a bolus intravenous injection of 0.2 mmol/kg of Gd-DTPA. Simultaneous measurements of regional blood flow were made using the radioactive microsphere method.

Results—After venous ligation, there was a 25% to 45% decrease in the degree of enhancement compared with preligation values on the ligated side. The decrease in cumulative enhancement (integrated over the entire time course) was statistically significant. The occlusion technique was verified by confirming a statistically significant decrease in blood flow determined by the microsphere method.

Conclusions—Dynamic Gd-DTPA-enhanced fast MRI technique can detect acute changes in bone marrow perfusion due to venous occlusion. This technique may have applications in the early detection of nontraumatic AVN.

Keywords

avascular necrosis; dynamic magnetic resonance imaging; femur; gadolinium-DTPA; magnetic resonance imaging; venous occlusion

---

Magnetic resonance imaging (MRI) has greatly improved diagnostic accuracy in the detection of avascular necrosis (AVN).[1] Although MRI is now considered highly sensitive, very early signs of AVN, if present, are subtle and nonspecific, such as diffuse marrow edema,[2] when conventional spin-echo technique is used. Because early surgical intervention, such as core decompression and rotational osteotomy, may improve the prognosis and prevent significant disability, improvement in current diagnostic capabilities is highly desirable.[3] In addition, reversal of iatrogenic causes, such as administration of exogenous corticosteroids, may be possible with early detection.

In a previous study, we demonstrated that the use of gadolinium-enhanced dynamic MRI is feasible in assessing perfusion to bone marrow.[4] In a simple dog model after arterial occlusion, changes not visible on spin-echo MRI were observed. This simple arterial model may have some relevance in cases of AVN that develop as a result of direct arterial trauma, such as femoral neck fracture. However, in nontraumatic AVN, resulting from steroid use or alcoholism, for example, the precise pathogenesis in the majority of cases remains obscure, and the arterial model we developed is probably not directly applicable.

In fact, direct measurement of intraosseous pressure has shown in the past that an increased value is usually an associated finding in AVN, suggesting vascular congestion.[3,5] Furthermore, there is histologic evidence that fatty proliferation, probably leading to venous stasis, may be a consistently prominent feature in specimens showing osteonecrosis.[6] Therefore, in this study, we evaluated the sensitivity of the gadolinium-enhanced dynamic MRI technique in detecting vascular congestion in a dog model where acute venous obstruction was created in one femur. As in the previous study, an independent assessment of blood flow was made using the radioactive microsphere method. Because the two methods do not evaluate exactly the same quantities, the microsphere technique was used primarily to qualitatively ensure the efficacy of the venous occlusion technique.

Materials and Methods

Five adult dogs, weighing 27 to 32 kg, were used. After preparation of the animal, including the placement of a ligature around the veins, microsphere injections were made and MRI was performed (each of these steps is described in further detail below). Without removing the animal from the scanner, the ligatures were tightened to accomplish complete occlusion. MRI and microsphere injections were repeated. (Analysis of MRI data and microsphere blood flow determination also are given in detail below.)

Animal Preparation

The dogs were anesthetized with an intramuscular injection of acepromazine (1 mL/kg) followed by an intravenous injection of sodium pentobarbital (30 mg/kg) via a catheter placed in a brachial vein. Each dog was intubated with a cuffed endotracheal tube, and allowed to breathe spontaneously. Anesthesia was maintained with sodium pentobarbital introduced into the intravenous saline solution that was dripped continuously throughout the experiment. An 8-Fr pigtail catheter was placed into the left ventricle via the left carotid artery to monitor systemic arterial pressure, and was used to inject radioactive microspheres for regional blood flow determination. The lower abdomen was opened by a vertical incision. The left common iliac vein and left lateral circumflex vein were carefully isolated, and ligatures were placed around both veins without tightening. The long ends of the ligatures were tunneled through a tube to the exterior of the animal. The abdomen was closed by two suture layers. When it was time to occlude the vessels, the ligature was pulled to maximum resistance. Ligation of the vessels was confirmed by gross observation after all measurements had been made.

Magnetic Resonance Imaging

Imaging was performed using a whole-body system (Signa, General Electric, Milwaukee, WI) operating at 1.5 Tesla. A gradient-recalled pulse sequence (GRASS) (time resolution = 45 mseconds, echo time = 9 mseconds, and flip angle = 65°) was used. The flip angle was chosen by maximizing contrast between phantoms with T1 similar to estimated T1 values of canine hematopoietic marrow before and after gadolinium-DTPA (Gd-DTPA) administration. The time resolution value was determined by balancing two opposing constraints—a long enough value to maximize contrast and a short enough value to give high temporal resolution between successive scans.

The animal was placed in the supine position in the scanner with both the hip and the knee of the hindleg flexed using a custom-made positioning apparatus. Preliminary coronal images were obtained to define axial planes of interest. Two axial levels were selected: one at mid-femoral head, and the other 3 to 4 mm cephalad through the obliquely oriented femoral neck. Sequential axial GRASS images were obtained alternately at the two levels, using two excitations, 5-mm slice thickness, 256×128 matrix, and 24-to 26-cm field of view. Acquisition time of each image was 11.5 seconds (time resolution of 23 seconds for each level).

A set of 32 sequential images (16 at each level) were obtained initially. After the first two images, or 23 seconds after the beginning of data acquisition, 0.2 mmol/kg body weight of Gd-DTPA was injected into a brachial vein over 2 to 4 seconds. After approximately 2 minutes (required for reconstruction of the initial image set and represcription), another set of 32 images was obtained. The last image, therefore, was obtained approximately 14 minutes after gadolinium injection. The same MRI protocol was used before and after venous occlusion.

Blood Flow Measurement by Radioactive Microspheres

Details of the radioactive microsphere technique for measuring regional blood flow to bone marrow have been described previously.[7] In this study, four tracers were used: gadolinium[153], Sn^{113}, Ru^{103}, and Sc^{46}. Two isotopes were selected arbitrarily for injection before venous ligation, and the remaining two were used after occlusion. The number of microspheres averaged 5×10^6 per injection. Injection was into the left ventricle via a catheter placed in a carotid artery. Reference samples were withdrawn from the left brachial artery using a calibrated Harvard pump at a constant sampling rate of 2.06 mL/minute starting 30 seconds before and continuing for 5 minutes after injection of microspheres. The stability of the animal was verified by monitoring heart rate, arterial blood pressure, and core body temperature throughout the experiment. At the end of the experiment, the animal was killed with an overdose of pentobarbital and potassium chloride. Bilateral femora were sectioned, and samples from the femoral head and neck were obtained. The radioactivity of the specimens was measured by a Packard multi-channel scintillation gamma counter, and regional bone marrow flow rates were determined.

Data Analysis

Mean signal intensity (SI) values were computed from three user-defined circular regions of interest placed centrally in proximal and distal portions of the femoral head and the femoral neck (Fig. 1). Contrast enhancement after the administration of gadolinium was expressed in terms of percent enhancement defined as:

$$\text{percent enhancement} = ([SI - SI_0]/SI_0) \times 100,$$

where SI_0 is the baseline signal intensity before gadolinium administration. Curves for percent enhancement versus time after gadolinium injection were generated for all three anatomic regions. The same was repeated for data obtained after unilateral venous ligation. Total percent

enhancement was computed as the sum of percent enhancement for each time point (or as the area under the curve of percent enhancement versus time), and was used as an overall quantitative measure of enhancement. The values of total percent enhancement before and after venous occlusion were compared by computing the fractional change after venous ligation as:

$$\% \text{ change in total } \% \text{ enhancement } = \frac{O_{after} - O_{before}}{O_{before}} \times 100,$$

where () denote total percent enhancement.

The values for ligation (left) and control (right) sides were compared, and Student's *t* test was performed.

From the radioactive microsphere data, regional blood flow values to femoral head and neck were obtained. Comparison between the values before and after unilateral venous occlusion was made by computing:

$$\% \text{ change in flow } = \frac{(\text{flow})_{after} - (\text{flow})_{before}}{(\text{flow})_{before}} \times 100.$$

Total percent enhancement and microsphere regional flow data were compared, and correlation coefficients for linear regression were obtained for each dog by including all data before ligation and data for the ligation side after occlusion. Differences in values obtained before and after occlusion were considered statistically significant ($P < .05$).

Results

An axial T1-weighted spin-echo image at the level of the femoral head and neck is shown in Figure 2. The proximal portion of the femoral head has high SI, consistent with fatty epiphysis. The portion of the femoral head distal to the physical line and femoral neck have low-to-intermediate SI reflecting predominantly hematopoietic marrow. A dynamic sequence of axial GRASS images at the level of the femoral head and proximal neck is shown in Figure 3. Bilaterally symmetric enhancement after contrast administration is evident in the distal portion of the femoral head and in the femoral neck (Fig. 3A). No visually obvious enhancement is seen in the proximal portion of the femoral head. After unilateral venous ligation on the left side, bilateral enhancement is seen again with no visually perceptible differences between ligated and control sides.

The time courses of percent enhancement versus time after gadolinium injection are displayed in Figure 4 for each anatomic region, where the curves before and after unilateral ligation are compared. An initial relative fast rise in SI followed by a slower prolonged decrease characterize these curves. Enhancement is noted in the proximal femoral head, which was not visually evident on images in the window settings that emphasized enhancement in the distal femoral head and in the femoral neck. On the ligated side, the difference between pre- and post-ligation data is evident in all anatomic regions; there was 25% to 45% reduction in percent enhancement after venous occlusion. On the control side there are no appreciable changes after contralateral ligation.

Comparison of total percent enhancement before and after ligation is made in Figure 5, in terms of percent change in total percent enhancement (as defined in the Materials and Methods section). On the ligated (left) side, there was a statistically significant decrease for all three anatomic regions ($P = .005$, proximal femoral head; $P = .019$, distal femoral head; and $P = .020$, femoral neck), although these changes were difficult to detect visually on images, as stated

previously. The largest relative decrease occurred in the proximal femoral head. On the control side, no statistically significant changes were seen after contralateral ligation.

Regional blood flow data obtained by the radioactive microsphere technique are presented in Figure 6, in terms of the percent change after ligation, as defined in the Materials and Methods section. There was a statistically significant decrease after ligation on the occluded side ($P = .020$, femoral head; and $P = .001$, femoral neck). The apparent slight decrease on the control side was not statistically significant. Plots of total percent enhancement versus microsphere blood flow measurements are shown in Figure 7 for one dog. Correlation coefficients for linear regression for the five dogs are 0.86, 0.82, 0.73, 0.49, and 0.55, respectively.

Discussion

In recent years, dramatic advances have been made in the diagnosis of AVN using MRI. Focal areas of abnormal signal are commonly seen on spin-echo images in advanced cases, and the "double-line" sign is considered specific for osteonecrosis.[8] Early but nonspecific signs reported using MRI include diffuse increased signal on T2-weighted images, representing edema.[2] Also, premature conversion to fatty marrow may be an associated, if not central, finding in early AVN.[9] Normal results found using MRI, however, do not exclude AVN; histologically proven cases have been shown to appear normal using spin-echo MRI. Current and past diagnostic methods, including intraosseous pressure measurement, core biopsy, and intramedullary venography, can detect early AVN, but these techniques are invasive.[3]

Previously, we reported that unilateral arterial embolization results in visually perceptible and statistically significant change in enhancement on dynamic Gd-DTPA–enhanced MRI in a dog model.[4] Because conventional spin-echo images failed to detect differences between embolized and nonembolized sides, the dynamic technique represents an improvement in the sensitivity for detection of acute massive insult to bone marrow arterial supply. In fact, in a study of patients with a femoral neck fracture, no acute changes in marrow signal were demonstrated using conventional MRI.[10] Our previous encouraging results in animals, therefore, suggest that the dynamic MRI technique may be applicable in studying selected clinical cases for detection of early perfusion deficit secondary to direct arterial damage.

In the vast majority of the cases, however, AVN has a nontraumatic etiology, such as corticosteroids or alcoholism, and the precise pathogenesis is obscure. Although mechanisms of direct arterial shutdown have been proposed, including occlusion of small vessels due to vasculitis, microfracture, and end-arterial fat embolism, none of these have been proven to be dominant in the pathogenesis of nontraumatic AVN, and the process is most likely multifactorial.[6] In the past, direct measurement of intraosseous pressure has shown that an increased value is usually an associated finding in AVN,[3,5] suggesting the pathologic state of vascular congestion. The temporal or causative relationship of this finding to the development of the disease, however, is not clear. Furthermore, in a study using histologic samples from patients receiving corticosteroids and from patients with alcoholism, a proliferation of cancellous bone fat at the expense of myeloid tissue was observed, progressing to swelling and necrosis of the fat cells and virtual absence of vascular sinusoids.[6] Compression of vascular sinusoids causing venous stasis and ischemia was postulated as a mechanism leading to osteonecrosis.

In this study, we demonstrated that after unilateral occlusion of the major draining veins, there was a statistically significant decrease in the degree of enhancement on the occluded side. The total percent enhancement parameter was chosen because it can be readily computed from the raw data on SI versus time, and it reflects the cumulative effect of gadolinium distribution. In our previous work on arterial occlusion, the peak enhancement was the key parameter, because

it is a sensitive and convenient measure of the arterial inflow. It should be noted, however, that percent enhancement is not simply related to the gadolinium concentration in tissue; rather, it is a pulse-sequence–dependent complicated function of tissue relaxation times, which in turn are essentially inversely proportional to gadolinium.[4]

We observe that after venous ligation, the time course of SI is qualitatively similar to that before ligation, reflecting grossly its two-phase nature: rapid inflow of gadolinium into intravascular and extracellular space, and slower washout from the extracellular space. Although total percent enhancement is significantly decreased, the timing of the peak is not appreciably affected. It is reasonable to infer that in acute venous obstruction, increased back pressure appears to result primarily in diminished magnitude of inflow.

The efficacy of venous occlusion by our ligation technique was validated from the radioactive microsphere data, which demonstrated a statistically significant decrease in flow on the ligated side. There was a decrease on the contralateral side to a lesser extent, possibly due to the systemic effects of unilateral occlusion, but this change was not statistically significant. Generally, good-to-fair correlations exist between the MRI and microsphere data for each dog when preligation data are used, and even when postligation data for the ligated side are added (Fig. 6). Postligation data for the control side were not used, because of unknown systemic physiologic effects of ligation, which may be time-dependent and therefore affect MRI and microsphere data nonuniformly. Correlation coefficients are not as high as in the arterial study, presumably because diminished gadolinium accumulation in tissue after an arterial insult is more directly correlated with decreased arterial flow determined by a single-pass technique. Thus, we have demonstrated that a decrease in bone marrow perfusion secondary to acute venous occlusion can be documented by data obtained from dynamic gadolinium-enhanced MRI technique. Table 1 summarizes the difference between the dynamic MRI technique and conventional spin-echo MRI in the detection of the effects of acute venous and arterial occlusion. The comparison is based on the data of this study and our previous work.[4] Distinction has been made between changes that are visually apparent and changes that are statistically significant in quantitative analysis outlined in this article.

In humans, a major cause of nontraumatic AVN is the administration of exogenous steroids. Although AVN eventually develops in few patients treated with steroids, early diagnosis may permit an alternative treatment regimen, preventing this crippling complication. Based on this study, it is feasible that this MRI technique could be extended to detect early perfusion abnormalities before the development of signal changes visible on conventional MRI in patients at risk for AVN.

There are, however, limitations to extending this model to AVN in humans. First, no experimental animal model, including a venous occlusion model, has succeeded in producing chronic osteonecrosis. Second, although compromise in venous drainage is probably a factor in certain cases of nontraumatic AVN, it most likely would not develop acutely as in this model. Third, hematopoietic marrow has a relatively higher degree of contrast enhancement than fatty marrow, and it has been reported that patients with AVN may have premature conversion of red to yellow marrow.[9] Therefore, if the patient population of interest has prematurely fatty marrow, the sensitivity of this particular method may decrease. In such a case, a fat-suppressed sequence may be needed. Finally, one well-recognized problem with using a gradient-echo technique in bone is the loss of anatomic detail within marrow secondary to magnetic susceptibility effects. We expect that the optimal pulse sequence for marrow perfusion will be redefined with continued advance in MRI technology.

In summary, we have demonstrated in a simple dog model that acute venous occlusion produces detectable changes on dynamic Gd-DTPA-enhanced MRI. And, despite the above-mentioned

limitations of the model, the results of this study, coupled with those of the previously reported arterial study, make this MRI technique plausible as a sensitive, noninvasive method to monitor perfusion to bone marrow. A study involving human subjects, with a view toward applying it eventually to the diagnosis of early AVN, is currently under way.

References

1. Mitchell DG. Using MR imaging to probe the pathophysiology of osteonecrosis. Radiology 1989;171:25–26. [PubMed: 2928533]

2. Turner DA, Templeton AC, Selzer PM, Rosenberg AG, Petasnick JP. Femoral capital osteonecrosis: MR findings of diffuse marrow abnormalities without focal lesions. Radiology 1989;171:135–140. [PubMed: 2928517]

3. Hungerford, DS. The Hip, Proceedings of the 7th Opens Scientific Meeting of the Hip Society. St. Louis, MO: Mosby; 1979. Bone marrow pressure, venography, and core decompression in ischemic necrosis of the femoral head; p. 218-237.

4. Cova M, Kang YS, Tsukamoto H, Jones LC, McVeigh E, Neff BL, Herold CJ, Scott WW Jr, Hungerford DS, Zerhouni EA. Bone marrow perfusion evaluated with Gadolinium-enhanced dynamic fast MR imaging in a dog model. Radiology 1991;179:535–539. [PubMed: 2014306]

5. Hungerford DS, Lennox DW. The importance of increased intraosseous pressure in the development of osteonecrosis of the femoral head: Implication for treatment. Orthop Clin North Am 1985;16:635–654. [PubMed: 3903603]

6. Solomon L. Idiopathic necrosis of the femoral head: pathogenesis treatment. Can J Surg 1981;24:573–578. [PubMed: 7326618]

7. Jones LC, Niv Al, Davis RF, Hungerford DS. Bone blood flow in the femora of anesthetized and conscious dogs in a chronic preparation using the radioactive tracer microsphere method. Clin Orthop 1982;170:286–295. [PubMed: 7127959]

8. Mitchell MD, Kundel HL, Steinberg ME, Kressel HY, Alavi A, Axel L. Avascular necrosis of the hip: comparison of MR, CT, and scintigraphy. AJR 1986;147:67–71. [PubMed: 3487233]

9. Mitchell DG, Rao VM, Dalinka M, et al. Hematopoietic and fatty bone marrow distribution in the normal and ischemic hip: new observation with I. 5T-MR imaging. Radiology 1986;161:199–202. [PubMed: 3763867]

10. Speer KP, Spritzer CE, Harrelson JM, Nunley JA. Magnetic resonance imaging of the femoral head after acute intracapsular fracture of the femoral neck. J Bone Joint Surg 1990;72A:98–103. [PubMed: 2295679]
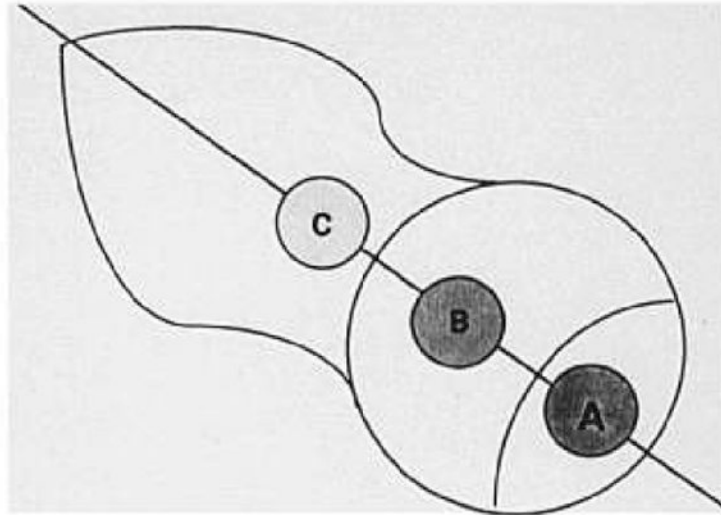
Fig. 1.
Diagram shows the regions of interest used in obtaining signal intensity: (A) proximal femoral head; (B) distal femoral head; and (C) femoral neck. The orientation is the same as in Figure 2.

Fig. 2.
An axial T1-weighted spin-echo image at the level of the femoral head and neck in a normal dog (TR/TE = 500/20). The orientation is the same as in Figure 1. Marrow is predominantly fatty in the proximal femoral head (small open arrow) and predominantly hematopoietic distal to the physeal line (large open arrow).
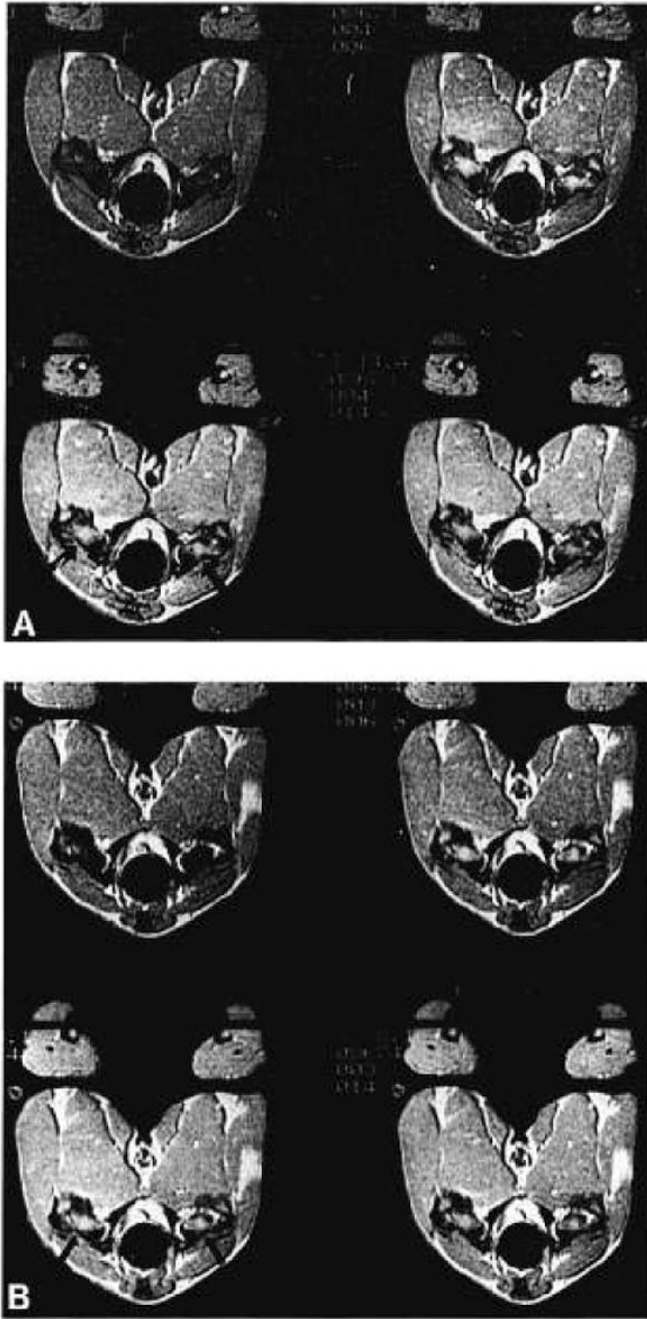
Figs. 3A and 3B.
Selected axial images at the level of the femoral head and neck in a normal dog after gadolinium-DTPA administration before (A) and after (B) venous occlusion on the left side. Images were obtained at 0 (top left), 46 (top right), 92 (bottom left), and 138 (bottom right) seconds after gadolinium administration. Bilateral enhancement is seen in the distal femoral head and femoral neck after contrast administration (arrows). After unilateral venous ligation, enhancement still appears bilaterally symmetric; however, quantitative analysis shows a statistically significant change (see Results section). Quantitative enhancement also is seen in the proximal femoral head (Fig. 3).
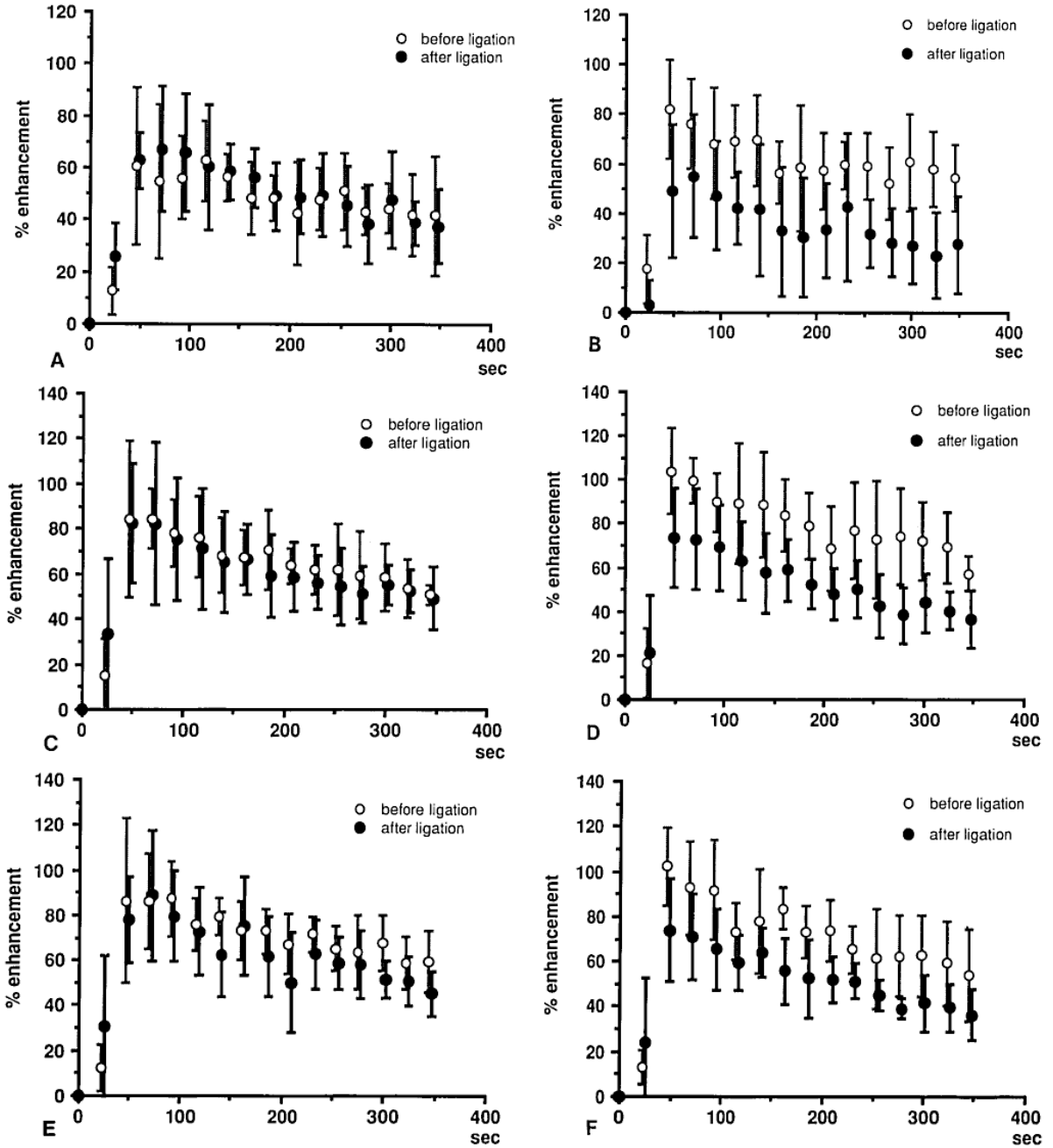
Figs. 4A-4F.

Percent enhancement versus time after Gd injection for each anatomic region. Curves before and after unilateral ligation are compared. A rapid rise followed by a slower decrease is seen. There is 25% to 45% reduction in percent enhancement after venous occlusion on the ligated side. Proximal portion of the femoral head on the right (control) (A) side and left (ligation) side. (B) Distal portion of the femoral head on the right (control) (C) side and left (ligation) (D) side. Femoral neck on the right (control) (E) side and left (ligation) (F) side.
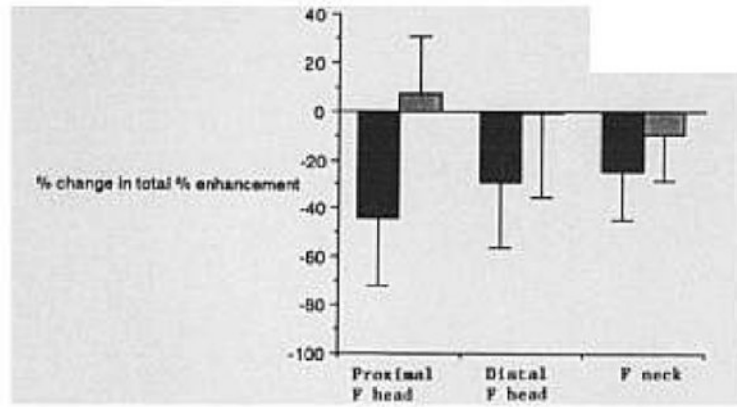
Fig. 5.
Percent change in total percent enhancement after ligation (see Methods section for definition).
A statistically significant decrease was noted for all three regions after ligation. The black bars
represent the left (ligation) side; the shaded bars represent the right (control) side.
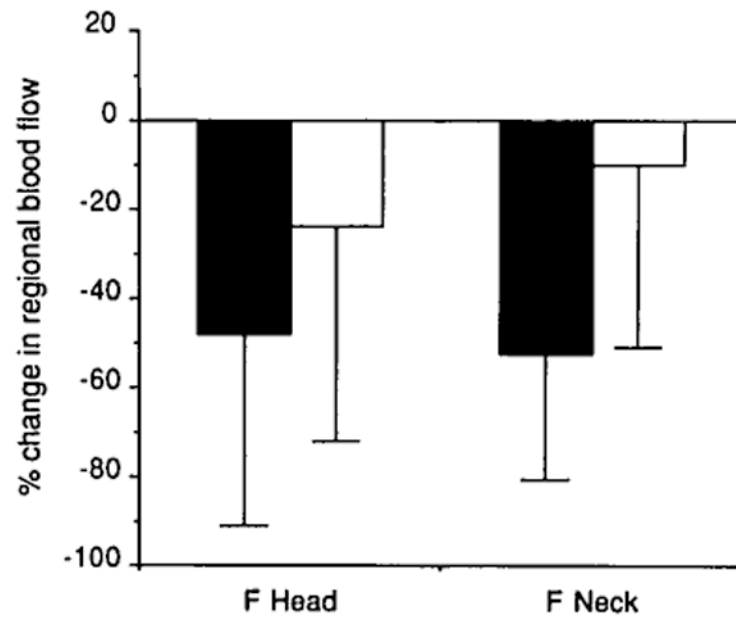
Fig. 6.
Percent change in regional blood flow after ligation determined by the radioactive microsphere method. The statistically significant decrease on the ligated side validates our occlusion method. Shaded bars represent the left (ligation) side; open bars represent the right (control) side.
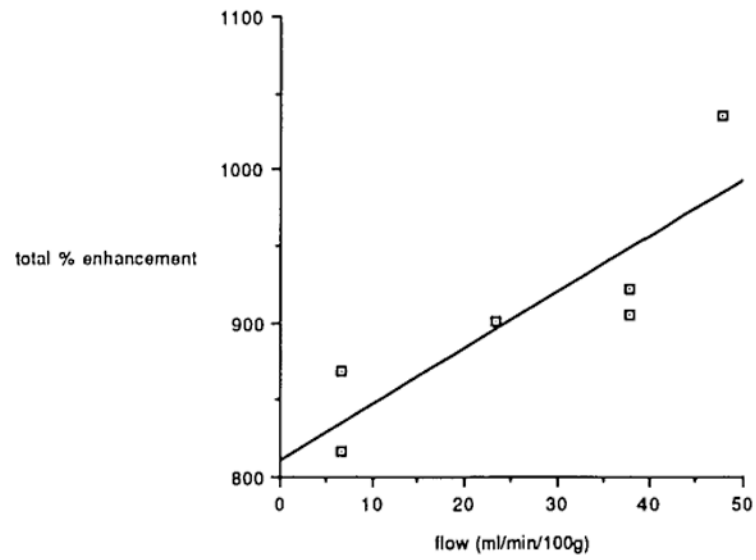
Fig. 7.
Magnetic resonance imaging total percent enhancement versus microsphere blood flow data for one dog. The correlation coefficient for linear regression for this dog is 0.86.

TABLE 1

Arterial versus Venous Ligation

	Spin-echo MRI	Dynamic MRI	Dynamic MRI with quantitative analysis
Effects of acute arterial occlusion	Not evident	Evident	Statistically significant
Effects of acute venous occlusion	Not evident	Difficult to see visually	Statistically significant

MRI: magnetic resonance imaging.